

# Study on the Blending Characteristics of Ternary Cementless Materials <sup>†</sup>

Yi-Hua Chang <sup>1</sup>, Lukáš Fiala <sup>2</sup> , Martina Záleská <sup>2</sup> , Dana Koňáková <sup>2</sup>, Wei-Ting Lin <sup>1,\*</sup>  and An Cheng <sup>1</sup><sup>1</sup> Department of Civil Engineering, National Ilan University, Ilan 26047, Taiwan<sup>2</sup> Department of Materials Engineering and Chemistry, Faculty of Civil Engineering, Czech Technical University in Prague, Thákurova 7/2077, 166 29 Prague 6, Czech Republic

\* Correspondence: wlin@niu.edu.tw; Tel.: +886-3-9317567; Fax: +886-3-9360125

<sup>†</sup> Presented at the 10th MATBUD'2023 Scientific-Technical Conference "Building Materials Engineering and Innovative Sustainable Materials", 19–21 April 2023.

**Abstract:** In this study, three industrial by-products (ultrafine fly ash, ground granulated blast-furnace slag (ggbs) and circulating fluidized bed co-fired fly ash) were used to produce ternary cementless composites without using alkali activators. The finenesses of ultrafine fly ash, ggbs and co-fired fly ash were 33,800, 5830 and 5130 cm<sup>2</sup>/g, respectively. The composite material was developed by mixing supplementary cementing materials of different particle sizes and exploiting the high-alkaline properties of the co-fired fly ash to develop a substantial hardening property like cement. The test specimens were made in the form of pastes and the water-to-cementitious-material ratio for the test was fixed at 0.55. The test results show that the flowability of the six different mixtures could be up to 120% and the setting time could be controlled within 24 h. At 60% of the ggbs proportion, the setting time could be held for 8 h. The compressive strength of each proportion reached 7 MPa at 7 days and 14 MPa at 28 days. The water-cured specimens exhibited better strength behavior than the air-cured specimens. Scanning electron microscopy found the main components of strength growth of the specimens to be hydrated reactants of C-A-S-H or ettringite. The results of the XRF analysis show that the specimens responded to higher compressive strengths as the Ca/Si and Ca/Al ratios increased.

**Keywords:** cementless composites; microscopic analysis; reactants; net-zero carbon emissions

**Citation:** Chang, Y.-H.; Fiala, L.; Záleská, M.; Koňáková, D.; Lin, W.-T.; Cheng, A. Study on the Blending Characteristics of Ternary Cementless Materials. *Mater. Proc.* **2023**, *13*, 9. <https://doi.org/10.3390/materproc2023013009>

Academic Editors: Katarzyna Mróz, Tomasz Tracz, Tomasz Zdeb and Izabela Hager

Published: 14 February 2023



**Copyright:** © 2023 by the authors. Licensee MDPI, Basel, Switzerland. This article is an open access article distributed under the terms and conditions of the Creative Commons Attribution (CC BY) license (<https://creativecommons.org/licenses/by/4.0/>).

## 1. Introduction

Cement production has become very energy-intensive, consuming more than 5% of the world's total energy demand, and a large portion of CO<sub>2</sub> emissions is associated with the cement industry [1]. However, cement concrete is widely used as a construction material due to its low cost and long service life. Although this material has high compressive strength and durability, its structural use is limited by the low tensile strength of the material and its susceptibility to crack expansion. In addition, the cement production process has a significant influence on global warming [2,3]. Presently, global production of Portland cement is approximately 4.6 billion tons per year. It is expected to reach a capacity of more than 6 billion tons by 2050 [4]. For countries around the world to achieve the goal of net-zero CO<sub>2</sub> emissions by 2050, there is an urgent need to find suitable substitutes for cement materials and significantly reduce cement usage [5], or to use alternative fuels, such as natural gas, biomass and agriculture-related secondary wastes (e.g., tires, sewage sludge, and municipal solid waste). This could significantly reduce indirect carbon emissions from burning fossil fuels or coal mines in heating rotary kilns [6]. Other strategies aim to use blended cement (such as ground granulated blast-furnace slag (ggbs), fly ash and other supplementary cementitious materials to replace cement) through the addition of cementitious materials; other chemical additives or aggregate types and grading optimization strategies may change the characteristics of concrete proportions and their environmental impact [5,7]. These strategies represent a significant research

area focused on developing methods to achieve the same material design parameters as those found in concrete structures using pure cement concrete but with a lower demand for Portland cement. The most effective approach is to completely replace cement with appropriate industrial wastes to achieve net-zero carbon emissions. This would significantly contribute to reducing emissions.

In this study, three industrial by-products were blended to completely replace cementitious materials without adding alkali activators to produce ternary cementless composites. After demolding, the test specimens were tested for cross-comparison of the compressive strength between air and water curing. The ternary cementless composites were tested using the flowability, setting time, X-ray fluorescence (XRF), and scanning electron microscopy (SEM) to verify their applicability and feasibility.

## 2. Experimental Details

### 2.1. Materials and Mix Proportions

This study used cementless materials made from ultrafine fly ash from thermal power plants, ggbs from continuously operating steel plants, and co-fired fly ash from circulating fluidized bed boilers. The finenesses of ultrafine fly ash, ggbs and co-fired fly ash were 33,800, 5830 and 5130  $\text{cm}^2/\text{g}$ , respectively. The specific gravity and chemical composition of the three raw materials were analyzed as described in Table 1, where ultrafine fly ash and ggbs are the amorphous-oriented materials. The tests were conducted on paste specimens, and the proportions are shown in Table 2, which shows that there were 6 mixtures of various proportions for a fixed water-to-cementitious-material ratio (w/c) of 0.55. After casting, the molds were removed once the specimens had hardened at room temperature for 24 h. After demolding, each group of mixtures was kept in water and exposed to air, respectively. Relevant tests were conducted when the test age was reached.

**Table 1.** The specific gravity and chemical compositions of the three raw materials.

Raw Materials	Specific Gravity	Chemical Compositions						
		CaO	SiO <sub>2</sub>	Al <sub>2</sub> O <sub>3</sub>	Fe <sub>2</sub> O <sub>3</sub>	SO <sub>3</sub>	MgO	Others
ultrafine fly ash	2.21	8.44	53.21	21.66	9.50	0.18	0.32	6.69
ggbs	2.88	40.24	33.68	14.37	0.29	0.66	7.83	2.93
co-fired fly ash	2.73	35.54	29.47	19.27	3.49	7.36	1.82	3.05

**Table 2.** Mix proportions (unit: g).

Mix No.	Ultrafine Fly Ash	ggbs	Co-Fired Fly Ash	Water
G1	0	500	500	550
G2	50	500	450	550
G3	0	600	400	550
G4	50	600	350	550
G5	0	400	600	550
G6	50	400	550	550

### 2.2. Test Procedures

The setting time tests were conducted using the Vicat Needle method following ASTM C191. The flow tests were conducted in accordance with ASTM C1437. Compressive strength tests were performed according to ASTM C109 for 7 and 28 days. The average value was measured after each of the three tests. The SEM observations were made on fragments left after the compression tests, and all the tests were carried out according to the procedures specified in ASTM C1723. XRF analysis was performed on the powder (about 5 g) produced in the compression test, and the test procedure was based on ASTM C1365.

### 3. Results and Discussion

#### 3.1. Flowability and Setting Time

The test results are summarized as shown in Table 3. The test results showed that the flowability of the specimen with a w/c of 0.55 exceeded the standard flowability (110%) for all groups. ggbs had better flowability when the ratio of ggbs to mixed fly ash reached 6:4. Using ultrafine fly ash instead of partially co-fired fly ash resulted in slightly lower flow values due to the ultra-fine particles. Only the final setting time was observed as a test indicator for cementless materials. Six groups were used to control the final setting time within 24 h. The final setting time can be significantly shortened to less than 8 h for specimens with a ggbs dosage up to 60% of the cementless blend. These test results were similar to those of the alkali-activated specimens with ggbs added. The setting time was accelerated when the ggbs exceeded 50%, meaning the setting times were dramatically reduced as the ggbs content increased [8,9].

**Table 3.** Results of flowability and setting time.

Mix No.	Flowability	Final Setting Time
G1	115%	21 h
G2	115%	24 h
G3	135%	8 h
G4	125%	7 h
G5	130%	21 h
G6	125%	20 h

#### 3.2. Compressive Strength

The results of the compressive strength tests at 7 and 28 days are shown in Table 4, including air and water curing. The test results showed that the strength of the water-cured specimens was better than that of the air-cured specimens, which demonstrated that this type of cementless material should be water-hardened. The hardening behavior of the ternary cementless materials was assumed to be due to the Ca-Si-Al colloidal system, and the strength development was due to calcium silicate hydrate (C-S-H) or calcium aluminum silicate hydrate (C-A-S-H) produced by the hydration process, which also supported the hypothesis that cementless materials could be made without alkali activators. The results were consistent with the results of previous tests [10,11]. The strength increased with hydration time, and the 28-day compressive strength of the specimens cured in water reached between 15 and 18 MPa. The cementless material had a specific compressive strength, which benefited a large number of industrial by-products, reduced the cement consumption, and reduced the carbon emissions.

**Table 4.** Results of compressive strength.

Mix No.	Compressive Strength (MPa)			
	Air Curing		Water Curing	
	7 Days	28 Days	7 Days	28 Days
G1	11.7	12.8	7.3	13.3
G2	6.4	13.7	8.6	15.6
G3	6.4	11.5	9.2	15.1
G4	6.1	11.0	12.1	15.0
G5	9.7	10.2	10.5	17.5
G6	10.2	11.1	9.8	16.4

#### 3.3. XRF Analysis

The results of the XRF analysis are shown in Table 5; the main chemical components of the cementless materials were found to be CaO, SiO<sub>2</sub> and Al<sub>2</sub>O<sub>3</sub>. The proportions of

the mentioned oxides were similar among the groups of specimens, which also indicated that the hydrated products should be C-S-H or C-A-S-H. It was noticed that the specimens all had a high content of  $\text{SO}_3$ , which quickly formed well-crystallized calcium-alumina crystals or ettringite in the voids of the specimens and helped to improve the hydrated bulk densities of the microstructures [12]. It may also be the leading cause of the higher compressive strength of G5 and G6 specimens (60% and 55% of co-fired fly ash). Moreover, the ratios of Ca/Si and Ca/Al in the air-cured and water-cured specimens were similar. The higher Ca/Si and Ca/Al specimens corresponded to better compressive strengths and represented more crystallization and gelation.

**Table 5.** XRF analysis.

Mix No.	Curing Type	Chemical Composition (%)				
		CaO	SiO <sub>2</sub>	Al <sub>2</sub> O <sub>3</sub>	Fe <sub>2</sub> O <sub>3</sub>	SO <sub>3</sub>
G1	Water	47.13	24.91	11.80	1.73	8.41
	Air	47.13	24.57	11.43	1.76	8.54
G2	Water	45.01	25.76	12.38	1.94	7.47
	Air	44.38	26.09	12.42	1.98	7.82
G3	Water	48.31	25.08	11.72	1.54	7.30
	Air	47.50	25.08	11.84	1.54	7.53
G4	Water	44.13	27.40	13.09	1.66	6.36
	Air	43.42	27.69	13.19	1.68	6.71
G5	Water	46.98	23.83	11.30	2.07	9.79
	Air	46.91	23.60	11.37	2.05	9.91
G6	Water	42.22	26.49	12.82	2.03	8.86
	Air	43.96	25.54	12.17	2.10	8.93

### 3.4. SEM Observation

The SEM photographs of each group of specimens are shown in Figure 1a–e. Many needle-like products (C-A-S-H or ettringite) could be seen on the surface of the microstructure of the specimen maintained in water. The needle-like hydration was more pronounced on the surface of the G1 specimen with lower strength, while hexagonal calcium hydroxide crystals were also observed on the surface of the G1 and G5 air-cured specimen. It was also indirectly stated that water curing was favorable for the continuous hydration of calcium hydroxide to produce C-S-H or C-A-S-H colloids. Figure 1e is an SEM photograph of the specimen with ultrafine fly ash, and transparent unreacted fly ash particles can be observed on its surface. It was clear that the reaction of ultrafine fly ash was favorable to the generation of C-A-S-H and ettringite. Figure 1f shows the experimental spectrum of SEM combined with energy dispersive X-ray (EDX) analysis for G5 water-cured specimen. It was found that elements with higher percentages were Si, Ca, Al, etc. It was evident that needle-like hydrates would contain C-S-H, C-A-S-H colloid, and calcium alumina, which was also the source of strength in the ternary cementless specimens.

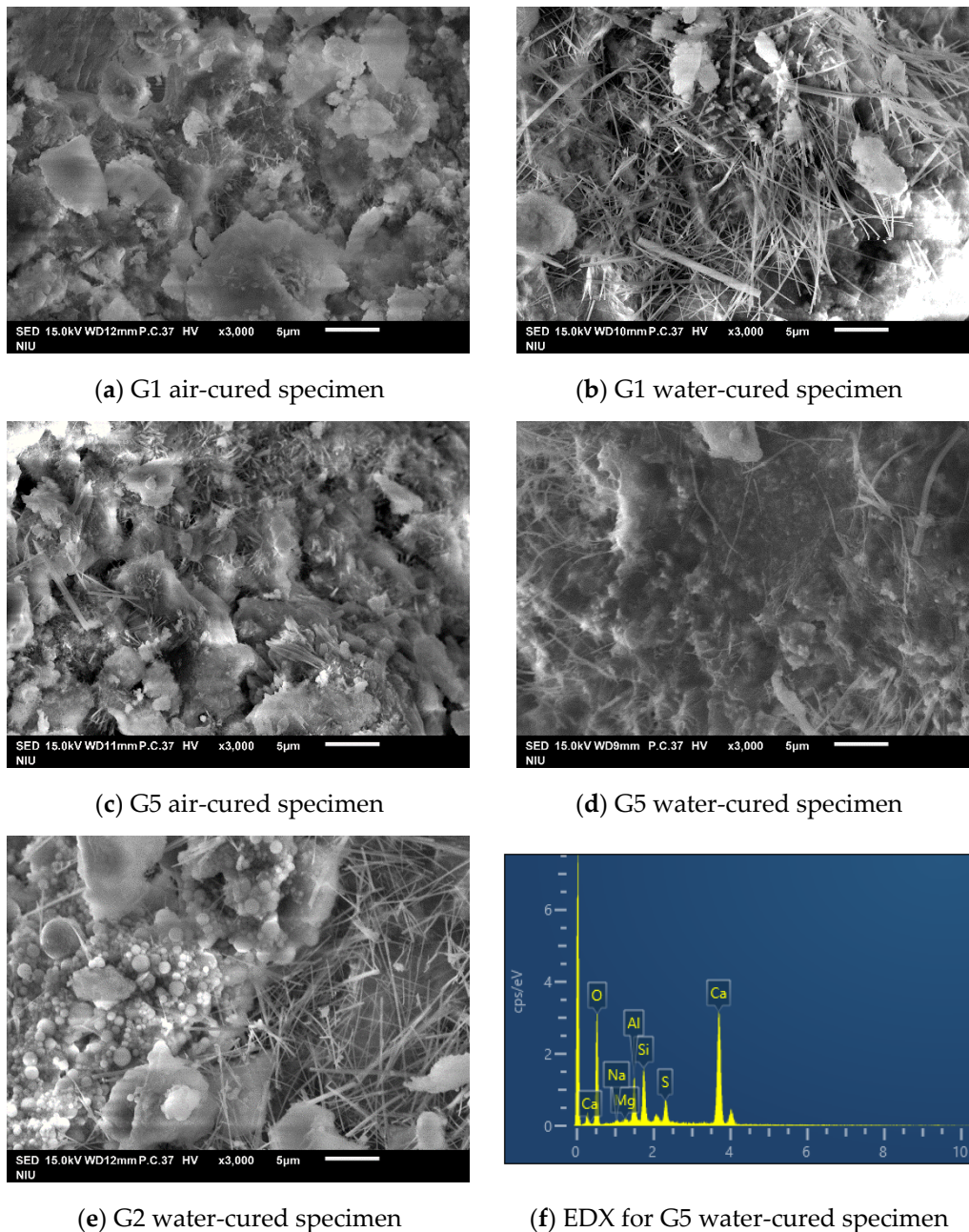


**Figure 1.** SEM photos (x3000).

#### 4. Conclusions

This study found that ternary cementless composites can be formed using ggbs, co-fired fly ash and ultrafine fly ash. The highest compressive strength was 17.5 MPa for two raw materials and 16.4 MPa for three raw materials. The average 28-day compressive strength ranged from 13 to 18 MPa, making it an innovative cementless material that meets net-zero carbon emissions. The cementless materials had better hydration and crystallization reactions when they were maintained in water, and the main products were C-S-H, C-A-S-H colloids and calcium alumina. These crystalline reactants can be verified using XRF, SEM and EDX analysis. The results also suggest that the novel ternary cementless composites developed in this study are worthy of further investigation into their engineering properties for future applications in construction materials.

**Author Contributions:** Conceptualization, W.-T.L. and Y.-H.C.; methodology, Y.-H.C.; validation, W.-T.L., Y.-H.C., M.Z. and D.K.; investigation, L.F.; resources, A.C.; data curation, M.Z. and D.K.; writing—original draft preparation, W.-T.L. and Y.-H.C.; writing—review and editing, W.-T.L. and L.F.; visualization, A.C.; supervision, W.-T.L. and L.F.; project administration, W.-T.L. and L.F.; funding acquisition, A.C. All authors have read and agreed to the published version of the manuscript.

**Funding:** The National Science and Technology Council (NSTC) in Taiwan supported this research with grant NSTC 111-2923-E-197-001-MY3 and the Czech Science Foundation in Czech Republic with project GAČR 22-00987J.

**Institutional Review Board Statement:** Not applicable.

**Informed Consent Statement:** Not applicable.

**Data Availability Statement:** Not applicable.

**Acknowledgments:** Publication cost of this paper was covered with funds of the Polish National Agency for Academic Exchange (NAWA): “MATBUD’2023-Developing international scientific cooperation in the field of building materials engineering” BPI/WTP/2021/1/00002, MATBUD’2023.

**Conflicts of Interest:** The authors declare no conflict of interest.

## References

1. Le Quéré, C.; Andrew, R.M.; Friedlingstein, P.; Sitch, S.; Pongratz, J.; Manning, A.C.; Jackson, R.B. Global carbon budget 2017. *Earth Syst. Sci. Data* **2017**, *10*, 405–448. [[CrossRef](#)]
2. Kawashima, A.B.; Martins, L.D.; Rafee, S.A.A.; Rudke, A.P.; de Morais, M.V.; Martins, J.A. Development of a spatialized atmospheric emission inventory for the main industrial sources in Brazil. *Environ. Sci. Pollut. Res.* **2020**, *27*, 35941–35951. [[CrossRef](#)] [[PubMed](#)]
3. Gil, A. Current insights into lignocellulose related waste valorization. *Chem. Eng. J. Adv.* **2021**, *8*, 100186. [[CrossRef](#)]
4. Andrew, R.M. Global CO<sub>2</sub> emissions from cement production, 1928–2018. *Earth Syst. Sci. Data* **2019**, *11*, 1675–1710. [[CrossRef](#)]
5. Miller, S.A.; John, V.M.; Pacca, S.A.; Horvath, A. Carbon dioxide reduction potential in the global cement industry by 2050. *Cement Concr. Res.* **2018**, *114*, 115–124. [[CrossRef](#)]
6. Chatziaras, N.; Psomopoulos, C.S.; Themelis, N.J. Use of waste derived fuels in cement industry: A review. *Manag. Environ. Qual. Int. J.* **2016**, *27*, 178–193. [[CrossRef](#)]
7. Amran, M.; Al-Fakih, A.; Chu, S.H.; Fediuk, R.; Haruna, S.; Azevedo, A.; Vatin, N. Long-term durability properties of geopolymers concrete: An in-depth review. *Case Stud. Constr. Mater.* **2021**, *15*, e00661. [[CrossRef](#)]
8. Xie, J.; Wang, J.; Rao, R.; Wang, C.; Fang, C. Effects of combined usage of GGBS and fly ash on workability and mechanical properties of alkali activated geopolymer concrete with recycled aggregate. *Compos. Part B* **2018**, *164*, 179–190. [[CrossRef](#)]
9. Nath, P.; Sarker, P.K. Effect of GGBFS on setting, workability and early strength properties of fly ash geopolymer concrete cured in ambient condition. *Constr. Build. Mater.* **2014**, *66*, 163–171. [[CrossRef](#)]
10. Lin, K.L.; Lin, W.T.; Korniejenko, K.; Hsu, H.M. Application of ternary cementless hybrid binders for pervious concrete. *Constr. Build. Mater.* **2022**, *346*, 128497. [[CrossRef](#)]
11. Li, C.; Zhang, N.; Zhang, J.; Song, S.; Zhang, Y. C-A-S-H gel and pore structure characteristics of alkali-activated red mud-iron tailings cementitious mortar. *Materials* **2022**, *15*, 112. [[CrossRef](#)] [[PubMed](#)]
12. du Toit, G.; van der Merwe, E.M.; Kruger, R.A.; McDonald, J.M.; Kearsley, E.P. Characterisation of the hydration products of a chemically and mechanically activated high coal fly ash hybrid cement. *Minerals* **2022**, *12*, 157. [[CrossRef](#)]

**Disclaimer/Publisher’s Note:** The statements, opinions and data contained in all publications are solely those of the individual author(s) and contributor(s) and not of MDPI and/or the editor(s). MDPI and/or the editor(s) disclaim responsibility for any injury to people or property resulting from any ideas, methods, instructions or products referred to in the content.